ACS OMEGA

http://pubs.acs.org/journal/acsodf

Article

Development and Validation of Small-Size Mechanism for RP-3 Aviation Fuel with High Precision

Shuanghui Xi, Junxing Hou, Shuai Yang, Zhenghe Wang, Shu-Hao Li,* and Fan Wang

Cite This: *ACS Omega* 2023, 8, 29150−29160

Read Online

ACCESS | Metrics & More | Article Recommendations | Supporting Information

ABSTRACT: In this study, a kerosene surrogate model fuel containing 73% *n*-dodecane, 14.7% 1,3,5-trimethylcyclohexane, and 12.3% *n*-propylbenzene (percentage in mass) is developed by considering both the physical and chemical characteristics of practical aviation kerosene. By combining the small-size C_0−C_4 (carbon number) core mechanism and the large hydrocarbon submechanisms, a low- and high-temperature chemical kinetic mechanism including 43 species and 136 reactions is constructed for the kerosene surrogate model fuel. The performance of the 43-species mechanism is validated by examining various experimental ignition delay times and laminar flame speeds of single component of *n*-dodecane and practical kerosene. The predicted main species concentrations during the oxidation process in the jet-stirred reactor by this small-size mechanism exhibit generally acceptable performance with the corresponding experimental data of RP-3 kerosene. The results of brute force sensitivity analysis indicate that the mechanism retains key reaction paths. This relatively small size can be applied to the simulation of computational fluid dynamics to further explore the practical problems of aviation fuel application in engine.

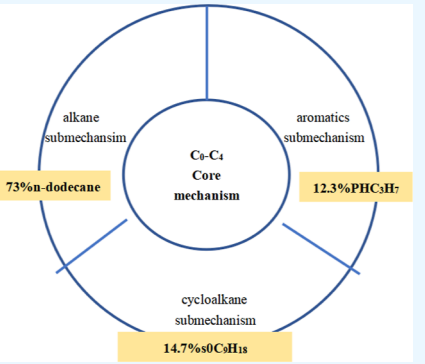

1. INTRODUCTION

The combustion of aviation fuel provides the necessary power for aircraft, while also increasing pollutant emissions. Currently, how to improve the combustion efficiency of fuel while reducing the emissions of pollutants is still the primary issue in the design of an aeroengine combustor. The numerical simulation of combustion by coupling the combustion reaction mechanism with computational fluid dynamics (CFD) provides an effective method for studying the combustion process and pollutant formation of an aeroengine.[1,2] It is helpful to optimize the design of an aeroengine combustor, explore the formation mechanism of pollution components, and greatly decrease the research cost. Therefore, the development of chemical reaction mechanisms that describe the combustion of aviation fuels has an important intentional value.

The practical aviation kerosene is usually composed of a large number of hydrocarbons, which is obviously unrealistic to construct a combustion mechanism for each of these components. Several studies indicated that alkanes, both *n*- and iso-alkanes, cycloalkanes, and aromatics are the major components of the aviation fuels certified.[3−8] Currently, multicomponent surrogate fuels that can reproduce the physical and chemical properties of practical aviation kerosene are commonly used to represent practical jet fuels.[3−12] The physical processes of fuel storage, flow, and heating can be modeled using physical characteristics. The chemical reaction processes of fuel cracking, ignition, and combustion can be modeled using chemical properties, including species concentrations, ignition delay time, and laminar flame speed.[13−15] Then, a detailed combustion mechanism of the practical fuel is constructed that based on these surrogate fuels.[16]

Shafer et al.[17] summarized the composition of Jet-A, Jet-A1, and JP-8 and pointed out that these three types of aviation kerosene have similar compositions. They are all composed of C_9−C_{16} large hydrocarbons with volume fractions of 20% *n*-alkanes, 40% isoalkanes, 20% cycloalkanes, and 20% aromatics, respectively. Based on these findings, many multicomponent surrogate models and their combustion mechanisms have been proposed.[18−21] RP-3 aviation kerosene is the main fuel of aeroengines in China, whose surrogate fuel mechanism have been widely researched, as shown in Table 1.

Although some surrogate fuel mechanisms have been developed based on practical aviation fuels, these mechanisms are limited to high-temperature combustion. Small molecules and alkyl peroxide radicals are the key reactions in high- and low-temperature, respectively.[30,31] These high-temperature mechanisms do not include such low-temperature reactions, so it is not possible to reliably describe the important combustion behavior at low temperatures. At present, the

Received: April 6, 2023
Accepted: July 26, 2023
Published: August 3, 2023

Table 1. Surrogate Fuels of RP-3 Kerosene and the Corresponding Reaction Mechanisms

researcher	surrogate fuel	reaction mechanism	verified property	temperature range
Zhang et al[22]	1,2,4-trimethylbenzene, *n*-decane	122 species, 900 reactions	ignition delay time	650−1500 K
Xu et al[23]	1/3/5-trimethylcyclohecane, *n*-dodecane, *n*-propylbenzene	138 species, 530 reactions	ignition delay time	1100−1500 K
Zhong and Peng[24]	*n*-dodecane, *n*-tetradecane, decalin	50 species, 274 reactions	laminar flame speed	high temperature
Mao et al[25]	toluene, isocetane, *n*-dodecane	223 species, 5689 reactions	ignition delay time	624−1437 K
Liu et al[26]	isododecane, 1,3,5-trimethylbenzene, *n*-decane	65 species, 200 reactions	species concentrations, ignition delay time, laminar flame speed	650−1400 K
Yu et al[27]	*n*-butylbenzene, *n*-dodecane, *n*-butylcyclohexane	1408 species, 8965 reactions	species concentrations, ignition delay time, laminar flame speed	625−1400 K
Liu et al[12]	1,3,5-trimethylcyclohexane, *n*-dodecane, *n*-propylbenzene	401 species, 2838 reactions	species concentrations, ignition delay time, laminar flame speed	700−1500 K
Liu et al[28]	*n*-dodecane, *n*-decane, isohexadecane, methylcyclohexane, toluene	121 species, 469 reactions	species concentrations, ignition delay time, laminar flame speed	1000−1700 K
Li et al[29]	*n*-dodecane, 2,2,4,4,6,8,8-heptamethylnonane, 2-methylheptane, decalin, o-xylene	2851 species, 12,242 reactions	ignition delay time	650−1250 K

Table 2. Comparison of the Physicochemical Properties between RP-3 and the Surrogate

fuel	density (g/cm^3)	viscosity (mm^2/s)	LHV (MJ/kg)	molecular weight (g/mol)	molar ratio of hydrogen-carbon
RP-3 kerosene	0.783[39]	1.55[40]	43.75[27]	150.03	2.05
surrogate model	0.782	1.62	43.7	154.2	2.03

research on the mechanism of low-temperature combustion of aviation kerosene surrogate fuel is still lacking.[22,25] Combustion is mainly low-temperature reaction when the initial combustion temperature is 600−1000 K. At the same time, low-temperature combustion is the key to reduce the emission of nitrogen oxides and other pollutants. Hydroperoxyalkyl (•ROOH) and its related radicals play a key role in the cold flame at low temperature. In addition, lean oil flameout is also an important problem to be solved in the design of aeroengine.[32] The low-temperature reaction path may also play an important role near the lean oil flameout limit.

In addition, it is difficult to adopt detailed or larger combustion mechanisms in numerical simulation of aeroengine. On the one hand, it takes much computation to combine the combustion mechanism with the flow equations for numerical solution because of a large number of species. On the other hand, larger span of different reaction time scales can also cause rigidity problem of calculation.[33] Therefore, generally only highly reduced combustion mechanisms can be used to the three-dimensional numerical simulation. Although some mechanism reduction methods have been developed,[30,34−38] it is still difficult to obtain a small-size reduction mechanism that accurately describes low-temperature combustion, starting directly with a very large and detailed mechanism that can reliably describe low-temperature combustion.

This paper describes a ternary-component surrogate model fuel of practical aviation kerosene that is based on considering both the main physical and chemical characteristics of the targeted kerosene. A 43-specise surrogate fuel mechanism with appropriate accuracy of RP-3 aviation kerosene which can describe low- and high-temperature in a wide range of conditions is then constructed using the small-size "core mechanism + submechanism", which is very practical skills for developing the chemical kinetic mechanism of practical kerosene. The mechanism is shown to provide reasonably key combustion characteristics compared with the experimental data, including the ignition delay times, laminar flame speeds, and major species mole fraction profiles under a wide range of pressures, temperatures, and equivalence ratios. Brute force sensitivity analysis is used to verify that the mechanism retains key reaction paths.

2. MECHANISM CONSTRUCTION

2.1. Selection of the Surrogate Model. There are many components in practical aviation kerosene, so it is impossible to construct the combustion mechanism for each component. Therefore, it is necessary to select some representative components of practical aviation kerosene that account for a relatively high proportion to construct the combustion mechanism based on "surrogate ideas".[17] Some key characteristics of practical aviation kerosene should be selected as the target for determining and optimizing the proportion of each surrogate component, and the physical and chemical properties of surrogate fuels should be close to those of practical aviation kerosene. The diffusion characteristics of gas-phase fuels depend on the molecular weight. In order to reproduce the diffusion characteristics of practical aviation kerosene in the gas-phase combustion, the average molecular weight of surrogate fuels should be close to that of practical aviation kerosene. The H/C ratio reflects the proportion of H_2O and CO_2 in the combustion products and determines the formation enthalpy of reaction and adiabatic flame temperature, which is an important characteristic parameter reflecting combustion rate and other combustion phenomena. Meanwhile, viscosity, density, and lower heating value (LHV) are also important physicochemical features of practical fuels. The main characteristic parameters of surrogate model and RP-3 kerosene in this article are shown in Table 2.

As alkanes, mono- and poly-aromatics and cycloalkanes are the three major compounds of jet fuels,[3−8] a mixture composed of 73.0% *n*-dodecane, 14.7% *n*-propylbenzene, and 12.3% 1,3,5-trimethylcyclohexane (percentage in mass)[23] is selected as surrogate fuel of RP-3 aviation kerosene to study its combustion kinetics.

https://doi.org/10.1021/acsomega.3c02335
ACS Omega 2023, 8, 29150−29160

2.2. Mechanism Construction of the Surrogate Model. *2.2.1. Construction of the Small-Size Core Mechanism.* The core mechanism of C_0−C_4 species is based on the USC-Mech II mechanism developed by Wang et al.,[41] which includes a detailed reaction mechanism of H_2/CO/C_1−C_4, including 111 species and 784 reactions. A large number of experiments have been conducted to verify the ignition delay time, laminar flame speed, and flame structure under a wide range of conditions. However, the size of this core mechanism is too large for CFD, let alone the size after being added with the submechanisms of the large hydrocarbons. Therefore, it is necessary to reduce the core mechanism while maintaining the accuracy of the mechanism. Sensitivity analysis and rate-of-production (ROP) are adopted to reduce the size of this mechanism in this paper.

According to our previous study,[30] the sensitivity analysis of species is adopted to determine the importance of that species in the mechanism. The sensitivity coefficient of every uncertain species will be determined, and the species with the smallest sensitivity coefficient will be deleted first. Sensitivity coefficients of the other species will change when a species is deleted from the mechanism. They are re-calculated each time when a species is removed. This procedure is iterated until the error of the obtained skeletal mechanism is larger than a given value. In addition, sensitivity analysis of reactions and ROP can further identify key reactions and species that affect the generation and consumption of surrogate components. The sensitivity analysis involved in this paper is aimed at the concentration of components during the combustion process, so the sensitivity coefficient is defined as follows

$$\text{sensitivity coefficient} = \frac{\alpha_i}{X_k^{\max}} \bullet \frac{\partial X_i}{\partial \alpha_I} \tag{1}$$

where α_i is the original reaction rate constant for the ith reaction and X_k is the concentration of species k. Based on the sensitivity coefficient, the key reactions that affect the concentration of important species can be determined, and the types of important reactions in the mechanism can be summarized.

ROP can directly provide information on the formation and consumption of a specified component during the entire combustion process or at a specific moment, and can quantitatively provide information on the reactions that affect the formation (P_A) or consumption (C_A) of a specified species A. The contribution of these reactions can be described by eqs 2 and 3. The contribution value of the ith reaction in the mechanism to the formation (P_{Ai}) or consumption (C_{Ai}) of species A at a certain time during the combustion process is defined as

$$P_{Ai} = \frac{\max(\nu_{A,i}, \omega_i, 0)}{P_A} \tag{2}$$

$$C_{Ai} = \frac{\max(-\nu_{A,i}, \omega_i, 0)}{C_A} \tag{3}$$

The above two mechanism analysis methods are used to determine the key species and important reaction paths of the core mechanism. The final core mechanism for the C_0−C_4 small molecules contains 25 species and 103 reactions, which are much fewer than that in the detailed mechanism.

2.2.2. Mechanism Construction of Small-Size Mechanisms of Large Hydrocarbons. The purpose of the small-size reaction network mechanism is to accurately reproduce the key combustion characteristics of practical aviation kerosene (such as ignition delay time and laminar flame speed) at the smallest possible mechanism size under wide conditions, so that the mechanism can be used for CFD numerical simulation. The representative components of the surrogate model are all large hydrocarbons. These large hydrocarbons will generate final small molecules after a series of chemical reactions, and their key reaction paths below C_4 are basically consistent. Therefore, the construction of the surrogate model mechanism should fully investigate the key species and reaction of *n*-dodecane, 1,3,5-trimethylcyclohexane, and *n*-propylbenzene. In order to reduce the final mechanism size, only the key species during the oxidation process are retained, without considering other isomers. At the same time, due to the largest proportion of *n*-dodecane among the three surrogates, only the critical low-temperature reaction of *n*-dodecane is considered.

The key low- and high-temperature reactions of *n*-dodecane and the key high-temperature reactions of 1,3,5-trimethylcyclohexane and *n*-propylbenzene in the mechanism are shown in Figure 1. For *n*-dodecane (RH), the radical R ($C_{12}H_{25}$) is

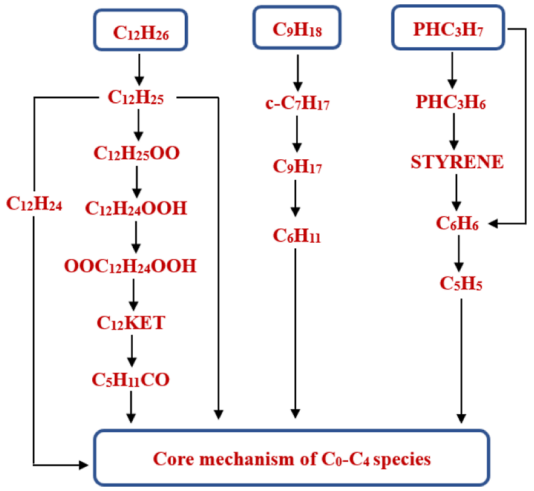

Figure 1. Overall reaction paths of each component in the surrogate fuel.

first generated through a hydrogen extraction reaction of O_2 and OH radicals. Under low temperature, R reacts with O_2 to generate RO_2, which is then isomerized to form QOOH. Then, QOOH reacts with O_2 to generate O_2QOOH. O_2QOOH is cracked to generate C_nKET, and C_nKET is then decomposed into smaller molecules.

At high temperatures, different fuels exhibit different oxidation behaviors due to the influence of their molecular structures. *N*-dodecane can pass through a series of β-scission reactions to generate C_0−C_4 components, which can also be directly decomposed into C_0−C_4 components through $C_{12}H_{24}$. In order to reduce the size of the mechanism, the continuous β-scission reactions are lumped into one reaction. For 1,3,5-trimethylcyclohexane, the c-C_9H_{17} radical can undergo decyclization to form C_9H_{17}. Then, C_9H_{17} is cracked to generate C_6H_{11}, which is further decomposed into C_0−C_4 components.

Due to the stability of the benzene ring, *n*-propylbenzene does not undergo reactions involving peroxy radicals at low temperatures. At high temperatures, the direct cracking of *n*-propylbenzene and the hydrogen extraction reaction are both

https://doi.org/10.1021/acsomega.3c02335
ACS Omega 2023, 8, 29150−29160

Table 3. Optimization of the Pre-exponent Factors of the Key Reactions

Reactions	original			revised		
	A	n	E	A	n	E
$OH + HO_2 = H_2O + O_2$	1.41×10^{15}	−1.76	60	1.41×10^{19}	−1.76	60
$C_2H_3 + O_2 = C_2H_2 + HO_2$	1.34×10^{3}	1.61	−383.4	1.34×10^{6}	1.61	−383.4
$C_2H_4 + OH = C_2H_3 + H_2O$	9.00×10^{8}	2	2500	9.00×10^{6}	2	2500
$C_2H_5 + HO_2 = CH_3 + HCHO + OH$	6.00×10^{11}	0	0	6.00×10^{13}	0	0
$aC_3H_5 + HO_2 = OH + C_2H_3 + HCHO$	6.60×10^{11}	0	0	6.60×10^{12}	0	0
$s0C_{12}H_{26} + O_2 = s2C_{12}H_{25} + HO_2$	5.50×10^{12}	0	27,800	7.00×10^{12}	0	27,800
$s2C_{12}H_{25} + O_2 = C_{12}H_{25}O_2$	3.00×10^{13}	0	0	3.00×10^{12}	0	0
$s2C_{12}H_{25} \rightarrow 2C_3H_6 + C_2H_5 + 2C_2H_4$	8.00×10^{13}	0	28,810	1.75×10^{13}	0	28,810

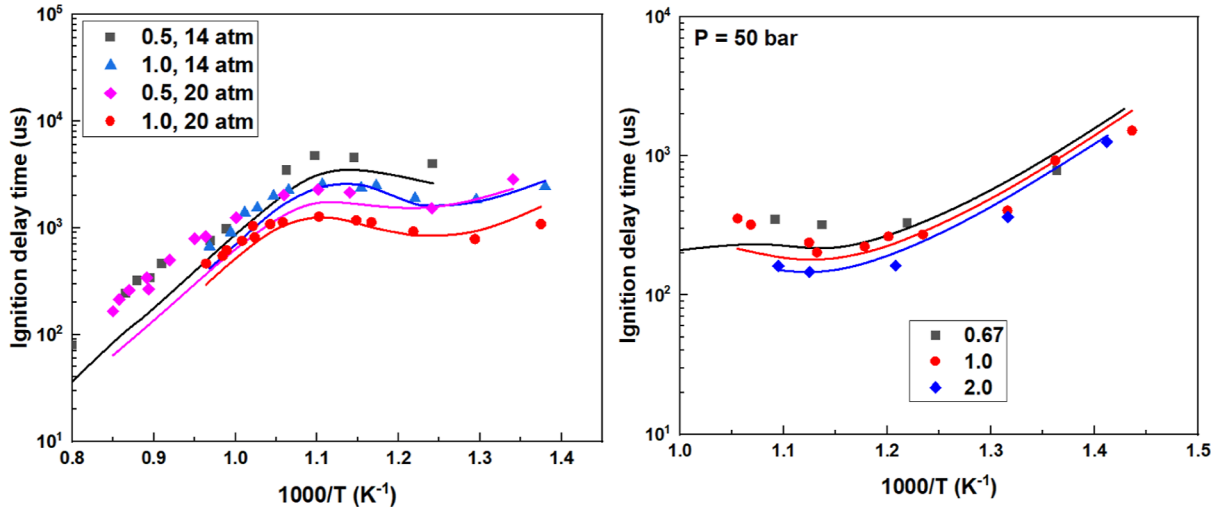

Figure 2. Variation of ignition delay times of *n*-dodecane with temperatures (symbol: experimental data and line: simulations).

relatively important reaction, which can generate PHC_3H_6 and benzene (C_6H_6). Then, C_6H_6 is ring-opened to form cyclopentadienyl (C_5H_5), and C_5H_5 undergoes subsequent reactions to generate C_0−C_4 components. PHC_3H_6 can pass through β-scission reaction to form STYRENE, and STYRENE undergoes a cracking reaction to generate C_6H_6 and C_2H_2. C_6H_6 undergoes related reactions to produce C_0−C_4 components.

Overall, the core mechanism of the C_0−C_4 species contains 25 species and 103 reactions, whereas the submechanism of *n*-dodecane, 1,3,5-trimethylcyclohexane, and *n*-propylbenzene contains 18 species and 33 reactions. Therefore, the final surrogate model mechanism includes 43 species and 136 reactions, which is provided in the Supporting Information. The kinetic data, thermodynamic data, and transport data for these species come from a study by Xu et al.[23] and Li et al.[29]

3. RESULTS AND DISCUSSION

3.1. Optimization of the Small-Size Surrogate Model Mechanism. Sensitivity analysis is adopted to select key reactions that have significant impact on the combustion characteristics of the mechanism and then to optimization of rate constants of these key reactions. A small-size mechanism with high precision suitable for CFD numerical simulation is obtained by adjusting the pre-exponent factors of the reaction rates. Key reactions and specific adjustment values are detailed in Table 3. The detailed optimization process is as follows:

(1) Preliminary estimation of the rate constants of key reactions based on detailed mechanisms;

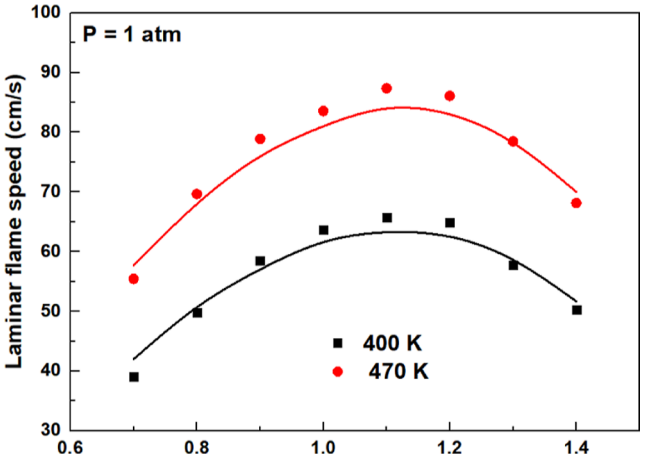

Figure 3. Variation of laminar flame speeds of *n*-dodecane with equivalence ratios (symbol: experimental data and line: simulations).

(2) The above reaction rate constants are optimized to enable the mechanism to accurately simulate the ignition characteristics under wide conditions;
(3) Sensitivity analysis of laminar flame speed for the mechanism obtained in step 2 is used to identify the key reaction that affects flame propagation and optimizes the rate constants to enable the mechanism to accurately simulate the flame propagation under wide conditions;
(4) Steps 2 and 3 are repeated until the final mechanism can well predict the ignition delay time in the shock tube and

https://doi.org/10.1021/acsomega.3c02335
ACS Omega 2023, 8, 29150−29160

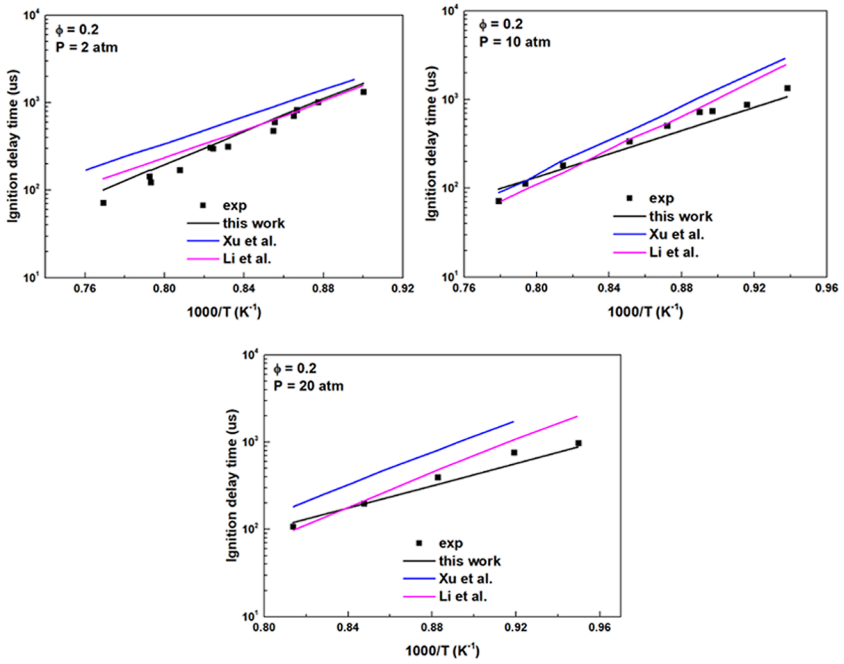

(a)

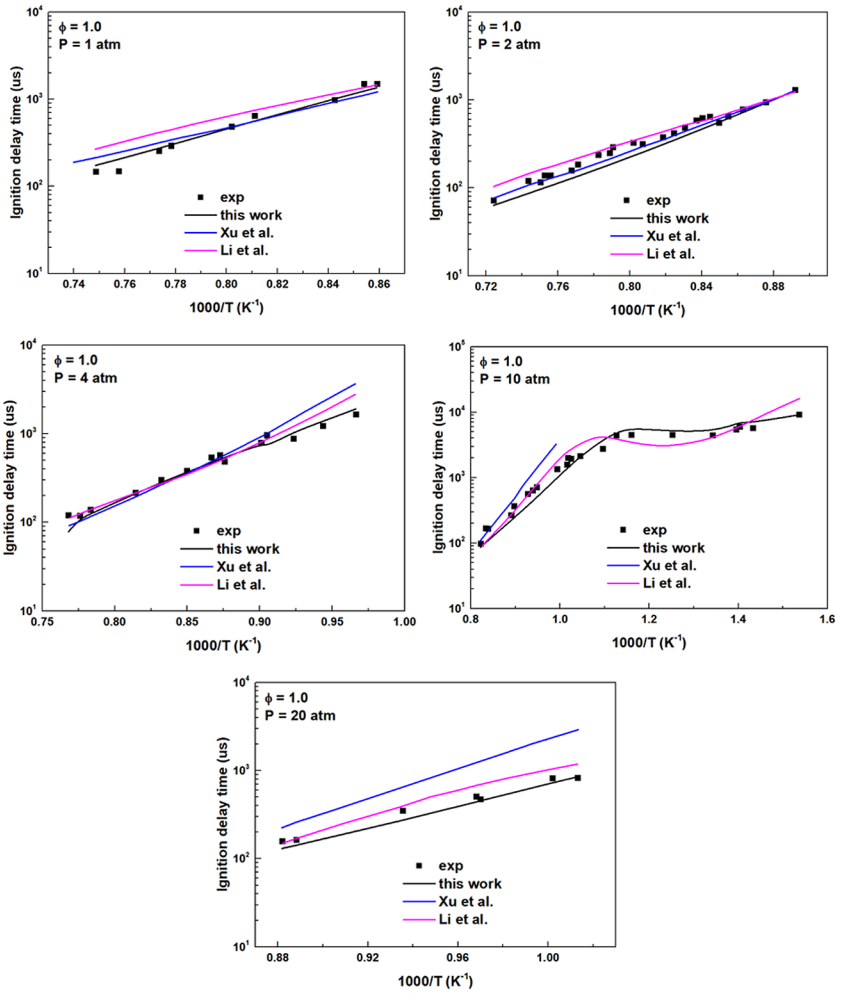

(b)

Figure 4. continued

https://doi.org/10.1021/acsomega.3c02335
ACS Omega 2023, 8, 29150−29160

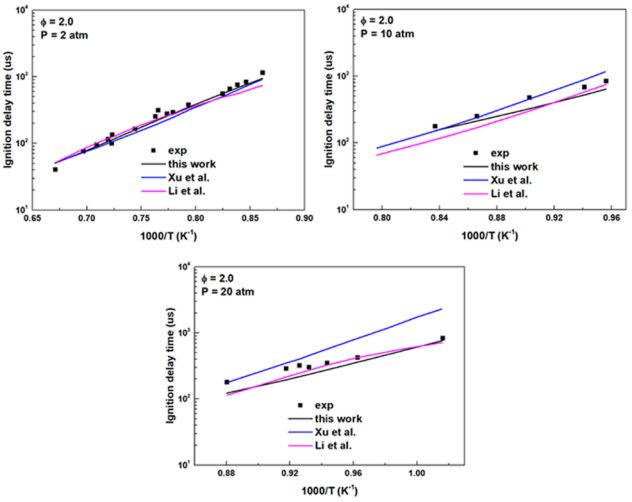

Figure 4. Variation of ignition delay times of RP-3 kerosene and surrogate models under various conditions: (a) ignition delay times at different pressures with ϕ = 0.2; (b) ignition delay times at different pressures with ϕ = 1.0; and (c) ignition delay times at different pressures with ϕ = 2.0. (symbol: experimental data and line: simulations).

the flame propagation speed in the one-dimensional premixed laminar flame under wide conditions.

3.2. Mechanism Verification. The ignition delay times and laminar flame speeds are widely used to verify the combustion reaction mechanism and are important indicators of reaction effectiveness.

Due to the largest proportion of *n*-dodecane in the surrogate model, the ignition delay times and laminar flame speeds of *n*-dodecane are verified by comparing with experimental data. At the same time, the important combustion characteristics of the 43-species mechanism are also further verified. The calculations are conducted using Chemkin-Pro software.[42]

3.2.1. Verification of the N-Dodecane Mechanism. 3.2.1.1. Verification of Ignition Delay times. The mechanism for *n*-dodecane employed in this work has been verified for ignition delay times under equivalence ratios of 0.5 and 1.0 and pressures of 14 and 20 atm as well as equivalence ratios of 0.67, 1.0, and 2.0 and the pressure of 50 bar. Reasonable results are achieved and compared with experimental data,[43−45] which is shown in Figure 2. It can be seen that the *n*-dodecane mechanism reasonably reproduces the ignition delay times and NTC phenomenon. Only the ignition delay times are slightly lower than the experimental data when the pressure is 14 atm and the temperature is greater than 950 K.

3.2.1.2. Verification of Laminar Flame Speeds. The mechanism for *n*-dodecane employed in this work has been verified for laminar flame speeds under inlet temperatures of 400 and 470 K and the pressure of 1 atm and compared with the experimental data.[46] The results are shown in Figure 3. It can be seen that the simulation results of the *n*-dodecane mechanism are in good agreement with the experimental results, and their largest differences are about 4.8 cm/s at an equivalence ratio of around 0.8. Laminar flame speed increases with the increase of initial temperature, which is consistent with the simulation results. The *n*-dodecane mechanism in the surrogate model can better provide simulation results of laminar flame speeds.

3.2.2. Verification of the Small-Size Surrogate Model Mechanism. 3.2.2.1. Verification of Ignition Delay times. In order to validate the obtained small-size reaction network mechanism, ignition delay times for the 43-species mechanism of this work, 138-species mechanism of Xu et al.,[23] and 2851-species mechanism of Li et al.[29] at different conditions are verified by comparing with experimental data.[22] Figure 4a−c shows the simulation results of the ignition delay time of these three RP-3 surrogate models at different temperatures and pressures with equivalence ratios of 0.2, 1.0, and 2.0, respectively. It can be seen from Figure 4a that the ignition delay times of the 138-species mechanism are longer than that of experimental data, but the 43-species mechanism and 2851-species mechanism generally agree well with the experimental data. In Figure 1b, ignition delay times of the 2851-species mechanism are larger than the experimental data with the pressure of 1 atm, and temperature is greater than 1250 K. Ignition delay times of the 138-species mechanism are significantly slower than the experimental data with the pressure of 20 atm. The 43-species mechanism reasonably reproduces ignition delay times compared with the experimental data at ϕ = 1.0. In addition, the 43-species mechanism and the 2851-species mechanism both reasonably reproduce the NTC phenomenon at low temperatures, and the 43-species mechanism agrees better with the experimental data. As shown in Figure 4c, ignition delay times of the138-species mechanism are slower than that of experimental data with the pressure of 20 atm, and temperature is less than 1050 K. Under other conditions, the results obtained by the three mechanisms are in good agreement with the experimental data. Among these results, the maximum ignition error of the 43 species mechanism is 36.15%, which appears at 1170 K and an equivalence of 0.2. Meanwhile, the maximum average error is 4.91%. Overall, the 43-species mechanism can reliably describe the ignition characteristics of RP-3 aviation kerosene at a wide range of temperatures and pressures with equivalence ratios of 0.2, 1.0, and 2.0.

3.2.2.2. Verification of Laminar Flame Speeds. In order to validate the obtained small-size reaction network mechanism, laminar flame speeds of the 43-species mechanism of this work and 138-species mechanism of Xu et al.[23] at different conditions are verified by comparing with those of experimental data. The mechanism of Li et al.[29] contains

https://doi.org/10.1021/acsomega.3c02335
ACS Omega 2023, 8, 29150−29160

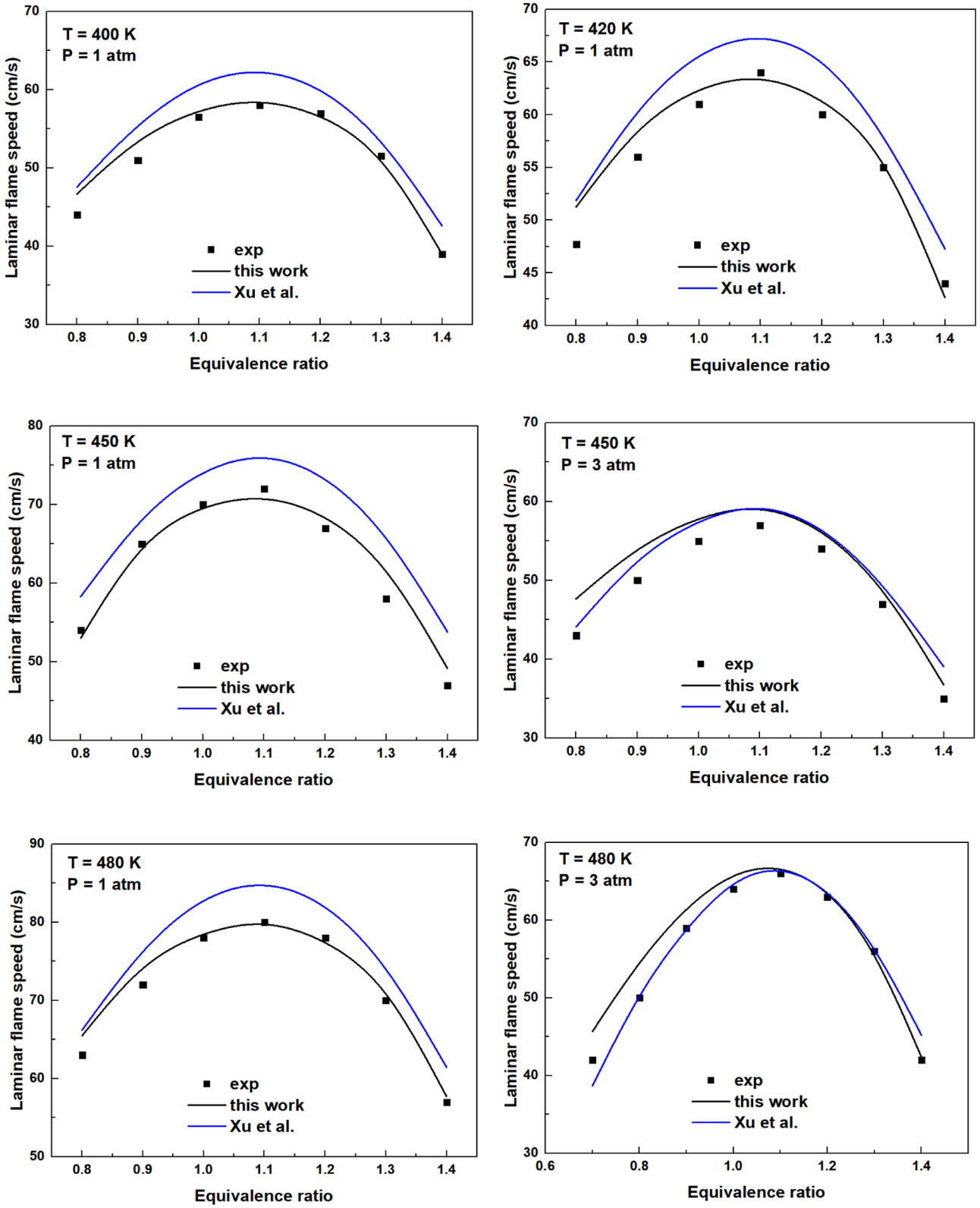

Figure 5. Variation of laminar flame speeds of RP-3 kerosene and surrogate models under various conditions (symbol: experimental data and line: simulations).

2851 species and 12,242 reactions, which cannot be used for simulation of laminar flame speeds due to the large number of species. The conditions for laminar flame speeds are P = 1 atm with inlet temperatures of 400, 420, 450, and 480 K as well as P = 3 atm with inlet temperatures of 450 and 480 K. The simulation results are shown in Figure 5. It can be seen that the trends of results given by the both mechanisms are consistent with that of experimental data. The laminar flame speed reaches its peak when the equivalence ratio is around 1.1. In addition, the laminar flame speed of the 138-species

https://doi.org/10.1021/acsomega.3c02335
ACS Omega 2023, 8, 29150−29160

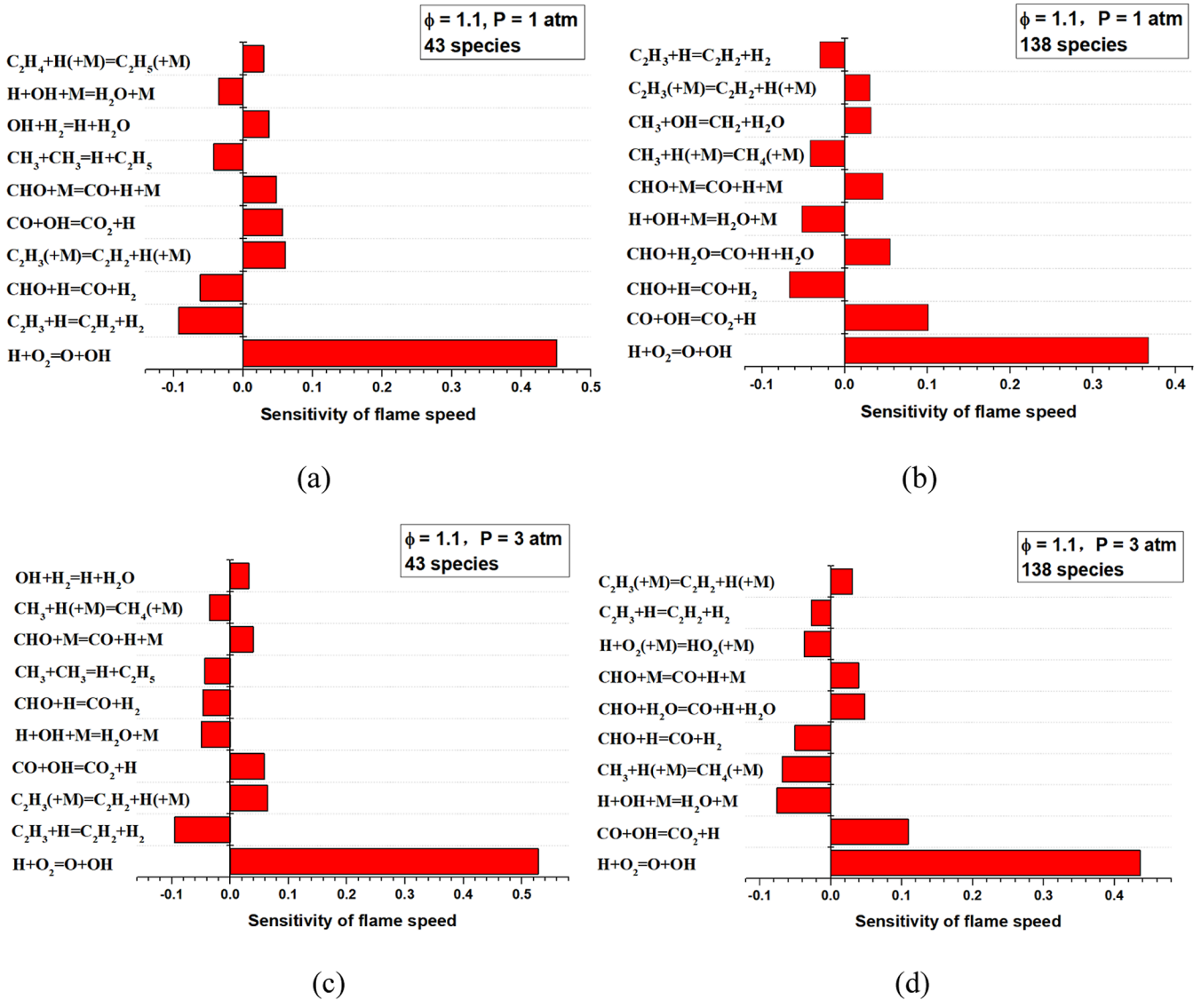

Figure 6. Sensitivity analysis of laminar flame speeds with the 43 species and 138 species mechanisms under various conditions: (a,c) sensitivity of flame speeds with the 43 species mechanism at different pressures with ϕ = 1.1; (b,d) sensitivity of flame speeds with the 138 species mechanism at different pressures with ϕ = 1.1.

mechanism agrees well with experimental results at P = 3 atm with temperatures of 450 and 480 K. However, it is faster than that of experimental data under other conditions. The laminar flame speed of the 43-species mechanism generally agrees well with experimental results, and the maximum error is less than 5 cm/s, which means a maximum error of 4.8%. The largest error occurs at P = 3 atm with the equivalence ratio of 0.8 and inlet temperatures of 480 K.

Results of sensitivity analysis on laminar flame speeds with the 43 species and 138 species mechanisms at pressures of 1 and 3 atm, an initial temperature of 450 K, and an equivalence ratio of 1.0 are illustrated in Figure 6. The equivalence ratio of 1.1 is the laminar flame speeds reach maximum at this temperature and pressure. A reaction with a positive sensitivity coefficient promotes flame propagation, while a reaction with a negative sensitivity coefficient suppresses flame propagation. It can be seen from this figure that key reactions on laminar flame speeds at these conditions with these two mechanisms are generally consistent. This confirms reliability of the 43 species mechanism in describing laminar flame speeds at these conditions. It can be seen from this figure that H + O_2 = O + OH is the most important reaction to promote flame propagation at these conditions. Overall, the 43 species mechanism can provide reasonable simulation results for laminar flame speed.

3.2.2.3. Verification of Species Concentration. To further verify the obtained 43-species mechanism, mole fractions of H_2, O_2, CH_4, CO, CO_2, and H_2O for RP-3/O_2/N_2 in jet-stirred reactor (JSR) with respect to temperature from the 43-species mechanism are compared with those of experimental data.[14] The conditions in JSR are P = 0.1 MPa, T = 550−1100 K, ϕ = 0.5, 1.0, and residence time of 2 s. Species profiles under these conditions are presented in Figure 7. It can be seen that the trends of mole fractions for H_2, O_2, CH_4, CO_2, and H_2O are basically consistent with the experimental data. However, generation and consumption of CO are both faster than RP-3 aviation kerosene.

3.2.2.4. Brute Force Sensitivity Analysis of the 43-Species Mechanism. Results of brute force sensitivity analysis on ignition delay times with the 43-species mechanism at

https://doi.org/10.1021/acsomega.3c02335
ACS Omega 2023, 8, 29150−29160

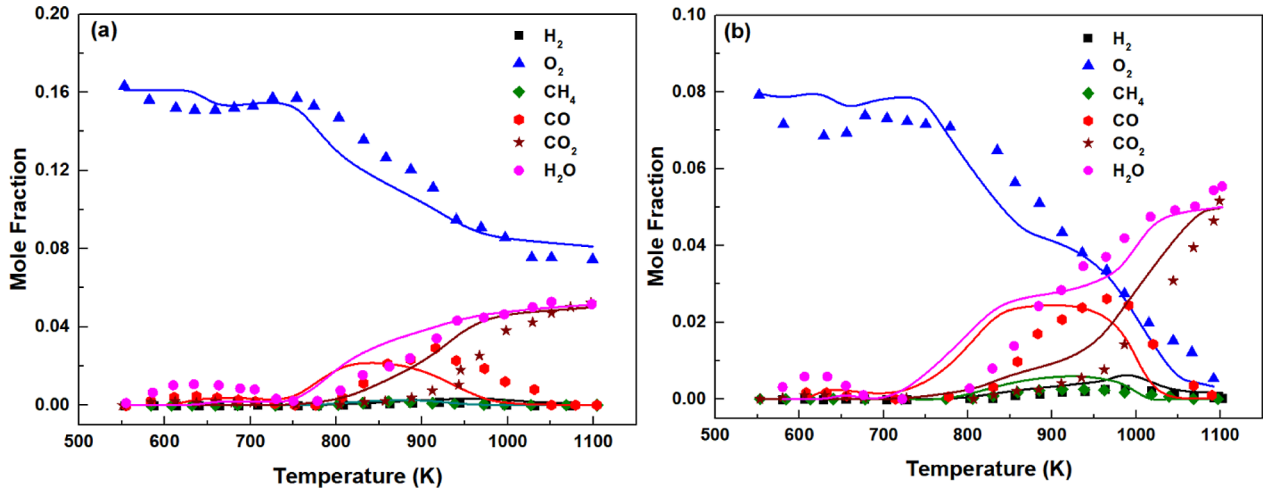

Figure 7. Variation of concentration profiles of RP-3 kerosene and the surrogate model in a JSR at 0.1 MPa, ϕ = 0.5, 1.0, and residence time of 2 s. (a) Variation of concentration profiles at P = 0.1 MPa and ϕ = 0.5 and (b) variation of concentration profiles at P = 0.1 MPa and ϕ = 1.0 (symbol: experimental data and line: the 43-species mechanism).

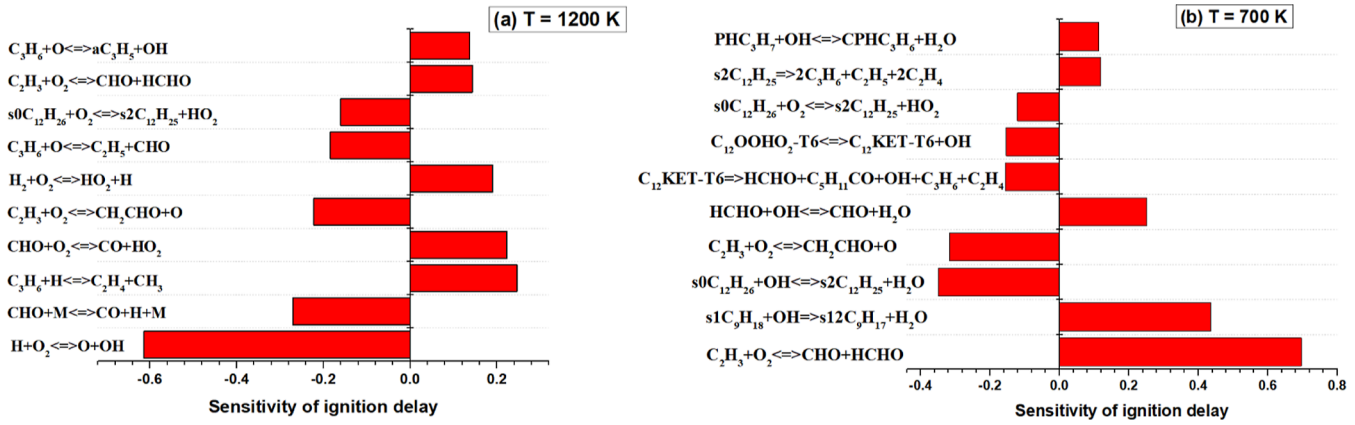

Figure 8. Brute-force sensitivity analysis for the surrogate model mechanism of 43-species at different temperatures with the pressure of 1 atm and equivalence ratio of 1.0.

temperatures of 1200 and 700 K, an equivalence ratio of 1.0, and a pressure of 1 atm are illustrated in Figure 8. It can be seen from Figure 8a that the key reactions that affect ignition are concentrated in small molecules or small radicals at high temperatures, which is consistent with the results by Xu et al.[23] As can be seen from Figure 8a, H + O_2 ↔O + OH is the most important reaction to promote ignition at T = 1200 K. This reaction is a chain branching reaction that produces O and OH radicals that promote the reaction. The most significant reaction to suppress ignition is C_3H_6 + H ↔ C_2H_4 + CH_3. The sensitivity analysis of the 43-species mechanism at low temperature 700 K is shown in Figure 8b. It can be seen from this figure that large hydrocarbons and related radicals have important effects on the self-ignition at low temperature. C_2H_3 + O_2 ↔ CHO + HCHO is the most important reaction to suppress self-ignition, while s0$C_{12}H_{26}$ + OH ↔ s2$C_{12}H_{25}$ + H_2O are the most important reactions to promote ignition at T = 700 K. Our results show that the sensitivity analysis of the surrogate model mechanism of 43-species can give reasonable results.

4. CONCLUSIONS

A ternary-component surrogate model fuel (73 mass % *n*-dodecane, 14.7% 1,3,5-trimethylcyclohexane, and 12.3% *n*-propylbenzene) has been proposed for practical aviation kerosene. This surrogate fuel can match well both the physical (molecular weight) and chemical (H/C ratio, ignition delay time, and laminar flame speed) characteristics of the targeted kerosene. Furthermore, a small-size mechanism (43 species and 136 reactions) with low- and high-temperature oxidation is developed based on the surrogate fuel. The aim of this mechanism is to mimic the key combustion characteristics of the kerosene ignition and flame, and it can be coupled to practical CFD simulations of the combustor. The mechanism has been widely validated using the experimental data for the ignition delay time and laminar flame speed of single components of *n*-dodecane and surrogate model, exhibiting generally acceptable performance. The species profiles in JSR with those of experimental results are further verified for the mechanism. The sensitivity analysis of the ignition delay time of the surrogate model fuel shows that large hydrocarbons and related radicals have important effects on the self-ignition at low temperatures, and the key reactions that affect ignition are concentrated in small molecules or small radicals at high temperatures. The chemical kinetic mechanism with few species and reactions constructed in this paper can be applied to further study of CFD simulations of practical combustors, providing more details of the practical combustion process.

https://doi.org/10.1021/acsomega.3c02335
ACS Omega 2023, 8, 29150−29160

■ ASSOCIATED CONTENT

Supporting Information

The Supporting Information is available free of charge at https://pubs.acs.org/doi/10.1021/acsomega.3c02335.

Reaction kinetics, thermodynamics, and transport data of 43-species mechanism (PDF)

■ AUTHOR INFORMATION

Corresponding Author

Shu-Hao Li − *School of Aero Engine, Zhengzhou University of Aeronautics, Zhengzhou 450046, P. R. China;* orcid.org/0000-0001-8077-6017; Email: piza123@126.com

Authors

Shuanghui Xi − *School of Aerospace Engineering, Zhengzhou University of Aeronautics, Zhengzhou 450046, P. R. China;* orcid.org/0000-0002-1699-464X

Junxing Hou − *School of Aerospace Engineering, Zhengzhou University of Aeronautics, Zhengzhou 450046, P. R. China;* orcid.org/0000-0002-7903-6692

Shuai Yang − *School of Aerospace Engineering, Zhengzhou University of Aeronautics, Zhengzhou 450046, P. R. China*

Zhenghe Wang − *School of Aerospace Engineering, Zhengzhou University of Aeronautics, Zhengzhou 450046, P. R. China*

Fan Wang − *Institute of Atomic and Molecular Physics, Sichuan University, Chengdu 610064, P. R. China;* orcid.org/0000-0001-7222-9734

Complete contact information is available at: https://pubs.acs.org/10.1021/acsomega.3c02335

Notes

The authors declare no competing financial interest.

■ ACKNOWLEDGMENTS

This work is supported by the Science and Technology Plan Project of Henan Province (232102320199, 222102320329, and 212102310093) and the Key Project of the Education Department of Henan Province (22A470010 and 23A460005). The authors thank for the help of the Center for Combustion Dynamics of Sichuan University.

■ REFERENCES

(1) Masiol, M.; Harrison, R. M. Aircraft engine exhaust emissions and other airport-related contributions to ambient air pollution: a review. *Atmos. Environ.* **2014**, *95*, 409−455.

(2) Li, J. R.; Liu, H. F.; Liu, X. L.; Ye, Y.; Wang, H.; Yao, M. Investigation of the combustion kinetics process in a high-pressure direct injection natural gas marine engine. *Energy Fuels* **2021**, *35*, 6785−6797.

(3) Dagaut, P.; Cathonnet, M. The ignition, oxidation, and combustion of kerosene: a review of experimental and kinetic modeling. *Prog. Energy Combust. Sci.* **2006**, *32*, 48−92.

(4) Dagaut, P.; Karsenty, F.; Dayma, G.; Diévart, P.; Hadj-Ali, K.; Mzé-Ahmed, A.; Braun-Unkhoff, M.; Herzler, J.; Kathrotia, T.; Kick, T.; et al. Experimental and detailed kinetic model for the oxidation of a Gas to Liquid (GtL) jet fuel. *Combust. Flame* **2014**, *161*, 835−847.

(5) Malewicki, T.; Gudiyella, S.; Brezinsky, K. Experimental and modeling study on the oxidation of Jet A and the n-dodecane/iso-octane/n-propylbenzene/1,3,5-trimethylbenzene surrogate fuel. *Combust. Flame* **2013**, *160*, 17−30.

(6) Braun-Unkhoff, M.; Riedel, U. Alternative fuels in aviation. *CEAS Aeronaut. J.* **2015**, *6*, 83−93.

(7) Riebl, S.; Braun-Unkhoff, M.; Riedel, U. A study on the emissions of alternative aviation fuels. *J. Eng. Gas Turbines Power* **2017**, *139*, 081503.

(8) Dong, Z.; Wei-Ming, Y.; Bei-Jing, Z. RP-3 aviation kerosene surrogate fuel and the chemical reaction kinetic model. *Acta Phys. Chim. Sin.* **2015**, *31*, 636−642.

(9) Mensch, A.; Santoro, R. J.; Litzinger, T. A.; Lee, S. Y. Sooting characteristics of surrogates for jet fuels. *Combust. Flame* **2010**, *157*, 1097−1105.

(10) Yan, Y. W.; Liu, Y. P.; Di, D.; Dai, C.; Li, J. Simplified chemical reaction mechanism for surrogate fuel of aviation kerosene and its verification. *Energy Fuels* **2016**, *30*, 10847−10857.

(11) Liu, Y. P.; Liu, Y. C.; Chen, D. B.; Fang, W.; Li, J.; Yan, Y. A simplified mechanistic model of three-component surrogate fuels for RP-3 aviation kerosene. *Energy Fuels* **2018**, *32*, 9949−9960.

(12) Liu, Y. X.; Richter, S.; Naumann, C.; Braun-Unkhoff, M.; Tian, Z. Y. Combustion study of a surrogate jet fuel. *Combust. Flame* **2019**, *202*, 252−261.

(13) Kim, D.; Martz, J.; Violi, A. A surrogate for emulating the physical and chemical properties of conventional jet fuel. *Combust. Flame* **2014**, *161*, 1489−1498.

(14) Liu, J.; Hu, E. J.; Yin, G. Y.; Huang, Z.; Zeng, W. An experimental and kinetic modeling study on the low-temperature oxidation, ignition delay time, and laminar flame speed of a surrogate fuel for RP-3 kerosene. *Combust. Flame* **2022**, *237*, 111821.

(15) Yi, R.; Chen, X.; Chen, C. P. Surrogate for emulating physicochemical and kinetics characteristics of RP-3 aviation fuel. *Energy Fuels* **2019**, *33*, 2872−2879.

(16) Mao, Y. B.; Yu, L.; Qian, Y.; Wang, S.; Wu, Z.; Raza, M.; Zhu, L.; Hu, X.; Lu, X. Development and validation of a detailed kinetic model for RP-3 aviation fuel based on a surrogate formulated by emulating macroscopic properties and microscopic structure. *Combust. Flame* **2021**, *229*, 111401.

(17) Shafer, L.; Striebich, R.; Gomach, J.; Edwards, T. Chemical class composition of commercial jet fuels and other specialty kerosene fuels. *14th AIAA/AHI Space Planes and Hypersonic Systems and Technologies Conference*, 2006.

(18) Honnet, S.; Seshadri, K.; Niemann, U.; Peters, N. A surrogate fuel for kerosene. *Proc. Combust. Inst.* **2009**, *32*, 485−492.

(19) Gutierrez-Antonio, C.; Gomez-Castro, F. I.; De Lira-Flores, J. A.; Hernández, S. A review on the production processes of renewable jet fuel. *Renew. Sustain. Energy Rev.* **2017**, *79*, 709−729.

(20) Narayanaswamy, K.; Pitsch, H.; Pepiot, P. A component library frame work for deriving kinetic mechanisms for multi-component fuel surrogates: application for jet fuel surrogates. *Combust. Flame* **2016**, *165*, 288−309.

(21) Alekseev, V. A.; Soloviova-Sokolova, J. V.; Matveev, S.; Chechet, I.; Matveev, S.; Konnov, A. Laminar burning velocities of n-decane and binary kerosene surrogate mixture. *Fuel* **2017**, *187*, 429−434.

(22) Zhang, C. H.; Li, B.; Rao, F.; Li, P.; Li, X. A shock tube study of the auto-ignition characteristics of RP-3 jet fuel. *Proc. Combust. Inst.* **2015**, *35*, 3151−3158.

(23) Jia-Qi, X.; Jun-Jiang, G.; Ai-Ke, L.; Jian-Li, W.; Ning-Xin, T.; Xiang-Yuan, L. Construction of auto-ignition mechanisms for the combustion of RP-3 surrogate fuel and kinetics simulation. *Acta Phys.-Chim. Sin.* **2015**, *31*, 643−652.

(24) Zhong, B. J.; Peng, H. S. Development of a skeletal mechanism for aviation kerosene surrogate fuel. *J. Propul. Power* **2019**, *35*, 645−651.

(25) Mao, Y. B.; Yu, L.; Wu, Z. Y.; Tao, W.; Wang, S.; Ruan, C.; Zhu, L.; Lu, X. Experimental and kinetic modeling study of ignition characteristics of RP-3 kerosene over low-to-high temperature ranges in a heated rapid compression machine and a heated shock tube. *Combust. Flame* **2019**, *203*, 157−169.

(26) Liu, X.; Wang, Y.; Bai, Y. Q.; Zhou, Q.; Yang, W. Development and verification of a physical-chemical surrogate model of RP-3 kerosene with skeletal mechanism for aircraft SI engine. *Fuel* **2022**, *311*, 122626.

(27) Yu, Z. Q.; Wei, S. L.; Wu, C. C.; Wu, L.; Sun, L.; Zhang, Z. Development and verification of RP-3 aviation kerosene surrogate fuel models using a genetic algorithm. *Fuel* **2022**, *312*, 122853.
(28) Liu, J.; Hu, E. J.; Zheng, W. L.; Zeng, W.; Chang, Y. A new reduced reaction mechanism of the surrogate fuel for RP-3 kerosene. *Fuel* **2023**, *331*, 125781.
(29) Li, A.; Zhang, Z. Y. N.; Cheng, X. G.; Lu, X.; Zhu, L.; Huang, Z. Development and validation of surrogates for RP-3 jet fuel based on chemical deconstruction methodology. *Fuel* **2020**, *267*, 116975.
(30) Xi, S. H.; Xue, J.; Wang, F.; Li, X. Reduction of large-size combustion mechanisms of n-decane and n-dodecane with an improved sensitivity analysis method. *Combust. Flame* **2020**, *222*, 326−335.
(31) Guo, J. J.; Li, S.; Tang, S.; Xiao, L.; Tan, N. Influence of different core mechanisms on low-temperature combustion characteristics of large hydrocarbon fuels. *Energy Fuels* **2019**, *33*, 7835−7851.
(32) Wang, H. R.; Jin, J. Overview of lean blowout limit prediction methods for aeroengine combustors. *Aeroengine* **2014**, *40*, 72−78.
(33) Bisetti, F. Integration of large chemical kinetic mechanisms via exponential methods with Krylov approximations to Jacobian matrix functions. *Combust. Theor. Model.* **2012**, *16*, 387−418.
(34) Lu, T. F.; Law, C. K. A directed relation graph method for mechanism reduction. *Proc. Combust. Inst.* **2005**, *30*, 1333−1341.
(35) Pepiot-Desjardins, P.; Pitsch, H. An efficient error-propagation-based reduction method for large chemical kinetic mechanisms. *Combust. Flame* **2008**, *154*, 67−81.
(36) Niemeyer, K. E.; Sung, C. J. Mechanism reduction for multicomponent surrogates: A case study using toluene reference fuels. *Combust. Flame* **2014**, *161*, 2752−2764.
(37) Liu, A. K.; Jiao, Y.; Li, S. H.; Wang, F.; Li, X. Y. Flux projection tree method for mechanism reduction. *Energy Fuels* **2014**, *28*, 5426−5433.
(38) Li, R.; Li, S. H.; Wang, F.; Li, X. Sensitivity analysis Based on intersection approach for mechanism reduction of cyclohexane. *Combust. Flame* **2016**, *166*, 55−65.
(39) Deng, H. W.; Zhang, C. B.; Xu, G. Q.; Tao, Z.; Zhang, B.; Liu, G. Z. Density measurements of endothermic hydrocarbon fuel at sub- and supercritical conditions. *J. Chem. Eng. Data* **2011**, *56*, 2980−2986.
(40) Deng, H. W.; Zhang, C. B.; Xu, G. Q.; Zhang, B.; Tao, Z.; Zhu, K. Viscosity measurements of endothermic hydrocarbon fuel from (298 to 788) K under supercritical pressure conditions. *J. Chem. Eng. Data* **2012**, *57*, 358−365.
(41) Wang, H.; You, X.; Joshi, A. V.; et al. USC Mech Version II. High-temperature combustion reaction model of H_2/CO/C_1-C_4 compounds.http://ignis.usc.edu/USC_Mech_II.htm.
(42) Reaction Design *Chemkin-Pro 15092*; Reaction Design: San Diego, 2009.
(43) Vasu, S. S.; Davidson, D. F.; Hong, Z.; Vasudevan, V.; Hanson, R. N-dodecane oxidation at high-pressures: measurements of ignition delay times and OH concentration time-histories. *Proc. Combust. Inst.* **2009**, *32*, 173−180.
(44) Shen, H. P. S.; Steinberg, J.; Vanderover, J.; Oehlschlaeger, M. A. A shock tube study of the ignition of n-heptane, n-decane, n-dodecane, and n-tetradecane at elevated pressures. *Energy Fuels* **2009**, *23*, 2482−2489.
(45) Yao, T.; Pei, Y. J.; Zhong, B. J.; Som, S.; Lu, T.; Luo, K. H. A compact skeletal mechanism for n-dodecane with optimized semi-global low-temperature chemistry for diesel engine simulations. *Fuel* **2017**, *191*, 339−349.
(46) Kumar, K.; Sung, C. J. Laminar flame speeds and extinction limits of preheated n-decane/ O_2/N_2 and n-dodecane/O_2/N_2 mixtures. *Combust. Flame* **2007**, *151*, 209−224.

https://doi.org/10.1021/acsomega.3c02335
ACS Omega 2023, 8, 29150−29160